



# Amperometric lactate nanobiosensor based on reduced graphene oxide, carbon nanotube and gold nanoparticle nanocomposite

Shabnam Hashemzadeh<sup>1</sup> · Yadollah Omid<sup>2,3</sup> · Hashem Rafii-Tabar<sup>1,4</sup>

Received: 19 April 2019 / Accepted: 27 August 2019 / Published online: 12 September 2019  
© Springer-Verlag GmbH Austria, part of Springer Nature 2019

## Abstract

A sensitive amperometric method is reported for the determination of lactate. A platinum electrode was modified with a composite prepared from reduced graphene oxide (rGO), carbon nanotubes (CNTs) and gold nanoparticles. The composite was synthesized by the in-situ reduction of gold(III) ions on the GO-CNT hybrid. Triple composite components showed synergistic effects on the enzyme loading, electrocatalytic activity and electron transfer between receptor and electrode surface. The amperometric lactate sensor was obtained by immobilization of lactate oxidase (LOx) on the modified electrode. LOx catalyzes the conversion of lactate into pyruvate and hydrogen peroxide. The generated hydrogen peroxide is simultaneously involved in the oxidation reaction, which is associated with the electron production. These electrons act as amperometric signal generators. At the low potential of 0.2 V, the nanobiosensor shows a relatively wide linear analytical range (i.e., 0.05–100 mM of lactate) with high electrochemical sensitivity ( $35.3 \mu\text{A mM}^{-1} \text{cm}^{-2}$ ) and limit of detection of 2.3  $\mu\text{M}$ . The sensor is stable, repeatable and reproducible. It is a highly sensitive tool for the detection of lactate in biological samples under both normoxic and hypoxic conditions.

**Keywords** Amperometric technique · Carbon nanotube · Electrochemical biosensor · Enzymatic nanosensor · Gold nanoparticles · Hydrogen peroxide · Lactate oxidase · Nanocomposite · Reduced graphene oxide

## Introduction

Lactate is a key metabolite produced during glucose metabolism. Under the hypoxic condition in cancer cells, the increase

---

**Electronic supplementary material** The online version of this article (<https://doi.org/10.1007/s00604-019-3791-0>) contains supplementary material, which is available to authorized users.

---

✉ Yadollah Omid  
yomidi@tbzmed.ac.ir

✉ Hashem Rafii-Tabar  
rafi-tabar@nano.ipm.ac.ir

<sup>1</sup> Department of Medical Physics and Biomedical Engineering, School of Medicine, Shahid Beheshti University of Medical Sciences, Tehran 19857-17443, Iran

<sup>2</sup> Research Center for Pharmaceutical Nanotechnology, Biomedicine Institute, Tabriz University of Medical Sciences, Tabriz 65811-51656, Iran

<sup>3</sup> Department of Pharmaceutics, Faculty of Pharmacy, Tabriz University of Medical Sciences, Tabriz 51666-14766, Iran

<sup>4</sup> The Physics Branch of the IRI Academy of Sciences, Tehran 19395-5531, Iran

in the rate of the glycolytic phenomenon is associated with the increasing conversion of pyruvate to lactate and its accumulation in the extracellular fluids of the tumor microenvironment (TME). Subsequently, these events can lead to metastasis and tumor progression [1–5]. An increased level of lactate concentrations within the TME is indeed considered as a criterion for the deviation in the pathway of glucose metabolism in cancer cells [6]. In addition to the clinical significance of lactate in various hypoxia-related diseases, it is an important biomolecule in biotechnology and food industry, which is also commonly used as an indicator for the quality assessment of food products [7].

To date, various analytical methods have been used for the detection of lactate, including optical [8] and electrochemical techniques [9, 10]. Further, enzyme-based electrochemical biosensors integrate the analytic capability of electrochemical approaches with the specificity of enzymes. In this line, enzymes, which are used as bio-receptor in lactate biosensors, are often lactate dehydrogenase (LDH) and lactate oxidase (LOx) [11–16].

Because of the necessity of lactate detection in a variety of samples with a wide range of lactate concentrations, it is

important to design a lactate sensor with high sensitivity and wide linear range. To reach this goal, it is necessary to load more enzyme molecules on the electrode surface. Alternatively, one of the tricks to increase receptor loading is the use of nanostructured materials for the modification of the surface of electrochemical sensors, which can lead to an increase in the surface-to-volume ratio, and improve the electrocatalytic and electron transfer activities. Different types of zero/one and or two-/three-dimensional nanostructures have been used to modify the surface of the electrochemical sensors [12, 14–21]. Graphene (Gr) and carbon nanotubes (CNTs) are the widely used nanomaterials for the development of electrochemical sensors, in large part due to their distinct properties such as high electrocatalytic and electron transfer activity, high surface/volume ratio, chemical stability and low cost [22, 23]. In addition to facilitating the electron transfer, the use of nanostructures such as gold nanoparticles (AuNPs) allows the adsorption of the enzyme molecules on the nanostructures while retaining their native conformation and catalytic activity [7, 20].

In this study, we report on the development of an electrochemical biosensor modified with a nanocomposite containing three types of nanostructures, reduced graphene oxide (rGO), CNTs and AuNPs (rGO-CNT-Au) for the detection of lactate in biological and food samples. We assumed that the components of the composite used to engineer the sensor might result in a synergistic effect on the immobilization of biomolecule, improve the electrocatalytic activity and electron transfer and provide a possibility for rapid amperometric detection of lactate in biological samples under both normoxic and hypoxic conditions as well as food samples.

## Materials and methods

### Materials

Gold(III) chloride trihydrate, L-(+)-lactic acid, lactate oxidase (from *Pediococcus* sp.,  $\geq 20$  U/mg), potassium hexacyanoferrate(III), potassium hexacyanoferrate(II) trihydrate, dopamine and uric acid were purchased from Sigma-Aldrich (St. Louis, USA, <http://www.sigmaaldrich.com>). Graphite, ascorbic acid, fructose and glucose were purchased from Merck (Darmstadt, Germany, <http://www.merck.com>). Carbon nanotube was purchased from US Research Nanomaterials Inc. (Houston, USA, <http://www.usnano.com>). Human epithelial A549 cell line (Code: C137) was purchased from Pasteur Institute (Tehran, Iran, <http://www.pasture.ac.ir>). The common chemicals used for the preparation of buffers were of analytical reagent grade. All the solutions were prepared using deionized distilled (DI) water.

### Instruments

Electrochemical measurements were performed by the Metrohm Autolab potentiostat/galvanostat system, PGSTAT302N (Metrohm Autolab, Herisau, Switzerland, <http://www.metrohm-autolab.com>) using NOVA 1.8 software for data processing, at ambient temperature. A common three-electrode system, with a modified Pt electrode (2 mm diameter) as the working electrode was employed. Auxiliary and reference electrodes were Pt wire and Ag/AgCl electrodes, respectively. The UV-Vis absorption spectra were recorded by a Cary-100 spectrophotometer (Varian, Australia, <http://www.varian.com>). The transmission electron microscopy (TEM) micrographs were accomplished by means of the LEO906E TEM (Carl Zeiss, Oberkochen, Germany, <http://www.zeiss.com>), operating with an accelerating voltage of 100 kV. The nanocomposite materials were characterized by the X-ray diffraction (XRD) using the Bruker D8 Advance (Bruker, Karlsruhe, Germany, <http://www.bruker.com>). The presence of elements was analyzed by the energy dispersive X-ray analysis (EDX) exploiting DSM-960A (Carl Zeiss, Germany, <http://www.zeiss.com>).

### Preparation of the rGO-CNT-Au nanocomposite

Graphene oxide (GO) was synthesized using a slightly modified Hummer's method [24]. Then, the GO-CNT hybrid was prepared according to the process reported by Hwa and co-workers [25]. Finally,  $\text{Au}^{3+}$  ions were reduced on the hybrid to form the rGO-CNT-Au nanocomposite [20]. The nanocomposite was then dispersed in N,N-dimethyl formamide (1 mg  $\text{mL}^{-1}$ ) and used for the modification of electrodes' surface.

### Fabrication and analysis of the modified Pt electrode with the rGO-CNT-Au nanocomposite

For cleaning, the Pt electrode surface was polished with alumina slurry and washed with nitric acid (2%) and water and dried using a nitrogen stream. About 3  $\mu\text{L}$  of the nanocomposite suspension was cast on the surface of the electrode in a drop-wise manner. After drying at the ambient conditions, 3  $\mu\text{L}$  LOx solution ( $\geq 20$  U, 10 mg  $\text{mL}^{-1}$  in phosphate buffer, pH = 7.5) was cast as a film onto the surface of the Au/CNT/rGO/Pt electrode, and then, the electrode was stored at 4 °C overnight. The modified electrode was rinsed with distilled water to remove excess LOx and stored at 4 °C prior to use. As the control, LOx was immobilized on the surface of the rGO and the rGO-CNT modified electrodes. Voltammetry was performed in the potential window of  $-0.4$ – $0.6$  V at the scan rate of 0.1  $\text{V s}^{-1}$ . The potential of 0.2 V was applied for all the amperometric experiments for a period of 100 s.

## Real samples preparation

The milk samples were diluted with the phosphate buffer at pH 7.5 (with a ratio of 1 to 2). The blood samples were taken from the veins of female volunteer before and after doing a 15 min physical exercise. The samples were sonicated for the lysis of blood cells and then centrifuged. The supernatant was diluted with the phosphate buffer (pH = 7.5) and used for the analysis.

The A549 cells were cultured in 5 mL RPMI supplemented with fetal bovine serum (10%) and penicillin-streptomycin (1%) in a tissue culture flask and incubated in normoxia (21% O<sub>2</sub>, 74% N<sub>2</sub> and 5% CO<sub>2</sub>) at 37 °C. The cells were passaged and divided into two equal parts and transferred to two flasks. After 48 h, one of the flasks was fed with a fresh cell culture media and the other was fed with N<sub>2</sub>-saturated medium to apply hypoxia, and the flask lid was completely covered in order to block the airflow into the flask. Then, both flasks were placed in an incubator at 37 °C for 24 h. Afterward, the contents of flasks were diluted with the phosphate buffer, transferred to the electrochemical cell and used as real samples for the detection of lactate in the normoxic and hypoxic conditions.

## Results and discussion

### Choice of materials

To investigate the effect of hypoxia on the production of lactate in cancer cells and its impacts on the metastasis and progression of cancer, we developed a novel rGO-CNT-Au

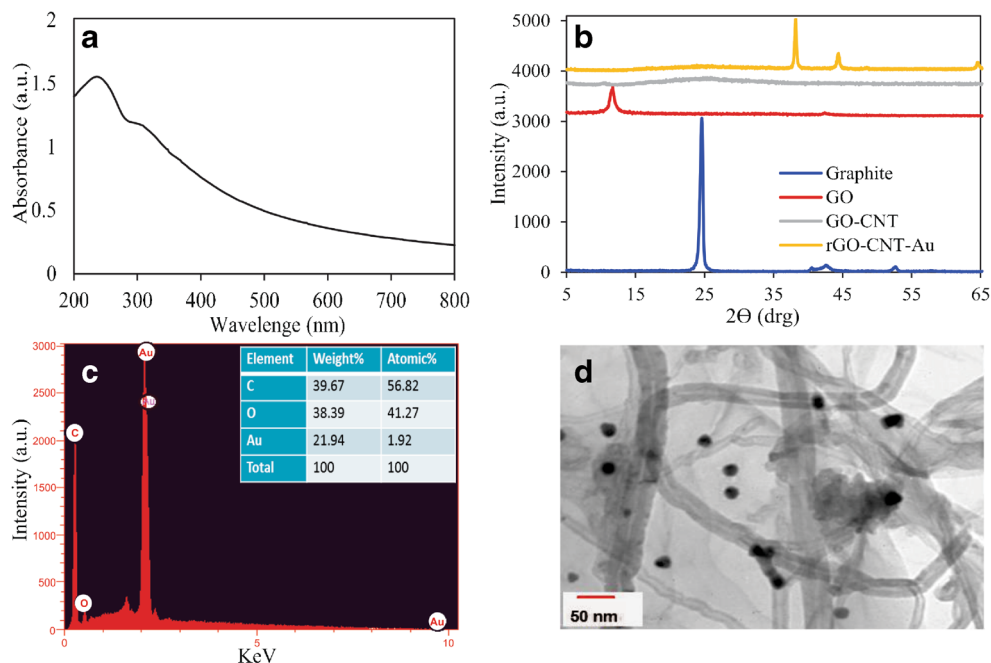
biosensor. Our main goal was to design a highly sensitive nanobiosensor to detect changes in the concentration of lactate induced by hypoxia in the biological samples. To achieve high sensitivity, a three-component nanocomposite was used to benefit from the synergistic effects of the components. For the selection of materials (i.e., AuNPs, CNTs and rGO), the most important criterion was the maximum electron transfer and enzyme loading capacities. AuNPs were selected to improve the electrocatalytic activity and loading of enzyme molecules on the surface of the electrode with the minimum effect on the function of the enzyme. Further, AuNPs and CNTs increase the sensitivity of the sensor due to their high conductivity. The rGO was used to provide the necessary platform for the interaction of AuNPs and CNTs in order to maximize the loading capacity with an improved electron transfer. The three-component nanocomposite was selected to maximize the sensitivity in a wide linear range. In addition, such three-component nanocomposite can provide a great possibility for further modifications and improvements.

### Characterization of the rGO-CNT-Au nanocomposite

The GO synthesis was confirmed with the appearance of a peak at 230 nm, corresponding to a  $\pi$ - $\pi^*$  plasmon peak, for the C-C aromatic bonds, and a shoulder around 300 nm, corresponding to the n- $\pi^*$  transitions of carbonyl groups, in the UV-Vis spectra (Fig. 1a) [24].

The comparison of the XRD pattern (Fig. 1b) of graphite and the GO exhibited the appearance of a sharp peak at  $2\theta = 11.3$  during interlayer spacing and oxidation. The GO-CNT hybrid network formation was characterized by the remove

**Fig. 1** Characterization of the nanocomposite **a** UV-Vis absorption spectrum of the GO nanosheets **b** The XRD images of graphite, GO, GO-CNT hybrid and the rGO-CNT-Au nanocomposite **c** The EDX spectra of the rGO-CNT-Au nanocomposite **d** The TEM micrograph of the rGO-CNT-Au nanocomposite



GO peak and the appearance of a weak and wide diffraction peak around  $2\theta = 26.1$ . The formation of this hybrid resulted from the strong  $\pi$  interaction between these two carbon nanostructures [25]. Finally, the XRD pattern of the rGO-CNT-Au nanocomposite confirmed the formation of the AuNPs on the rGO-CNT hybrid with the appearance of three peaks at  $2\theta = 38.2, 44.4, 64.6$ , respectively corresponding to Au (111), (200) and (220) reflections of crystalline Au (0) [20]. Based on the EDX spectra shown in Fig. 1c, the in situ synthesized AuNPs have made up 21.94% of the nanocomposite and the rest of the composite weight was roughly equal to carbon and oxygen. The microstructure of the nanocomposite was investigated by TEM. Figure 1d illustrates that the rGO-CNT networks provide an appropriate supporting substrate for the incorporation of the AuNPs (20–30 nm).

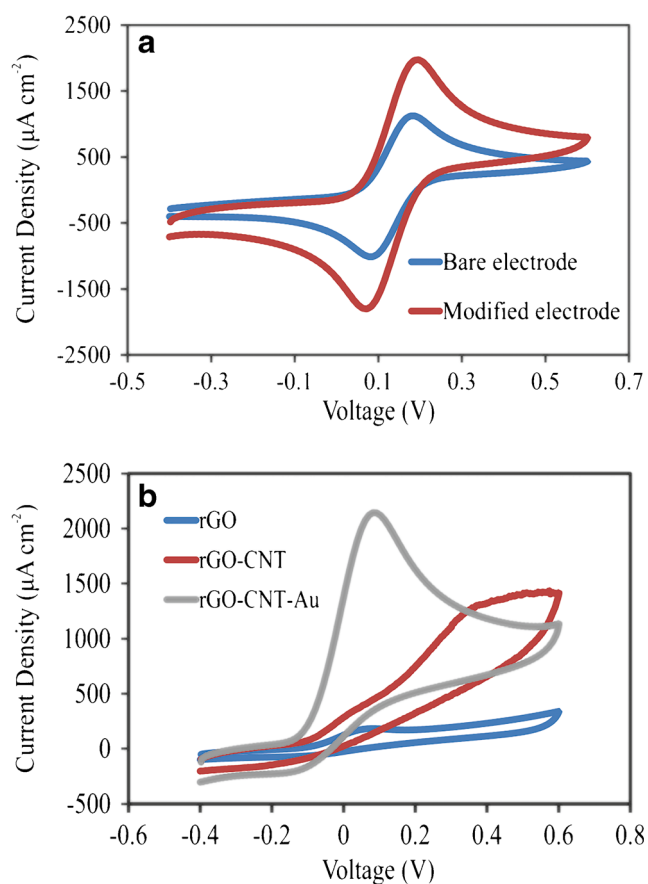


**Fig. 2** The electrochemical characterization of the nanocomposite **a** The CV analysis of the bare and modified electrodes in  $\text{K}_3\text{Fe}(\text{CN})_6/\text{K}_4\text{Fe}(\text{CN})_6$  (5 mM in 0.1 M KCl solution) **b** The CV analysis of the LOx/rGO/Pt, LOx/CNT/rGO/Pt and LOx/Au/CNT/rGO/Pt electrodes in the presence of 10 mM l-lactic acid in the phosphate buffer, pH = 7.5. Both analyses were performed at the potential window of  $-0.4$ – $0.6$  V and the scan rate of  $0.1 \text{ V s}^{-1}$

## Electrochemical characterization of the sensor

The effect of the electrode surface modification on electron transfer was investigated by the use of cyclic voltammetry technique in  $\text{K}_3\text{Fe}(\text{CN})_6/\text{K}_4\text{Fe}(\text{CN})_6$  (5 mM in 0.1 M KCl solution) between  $-0.4$ – $0.6$  V with a scan rate of  $0.1 \text{ V s}^{-1}$ . Figure 2a shows that the surface modification of the Pt electrode with the nanocomposite increase the peak current in the  $\text{Fe}(\text{CN})_6^{3-/4-}$ , as compared to the bare electrode.

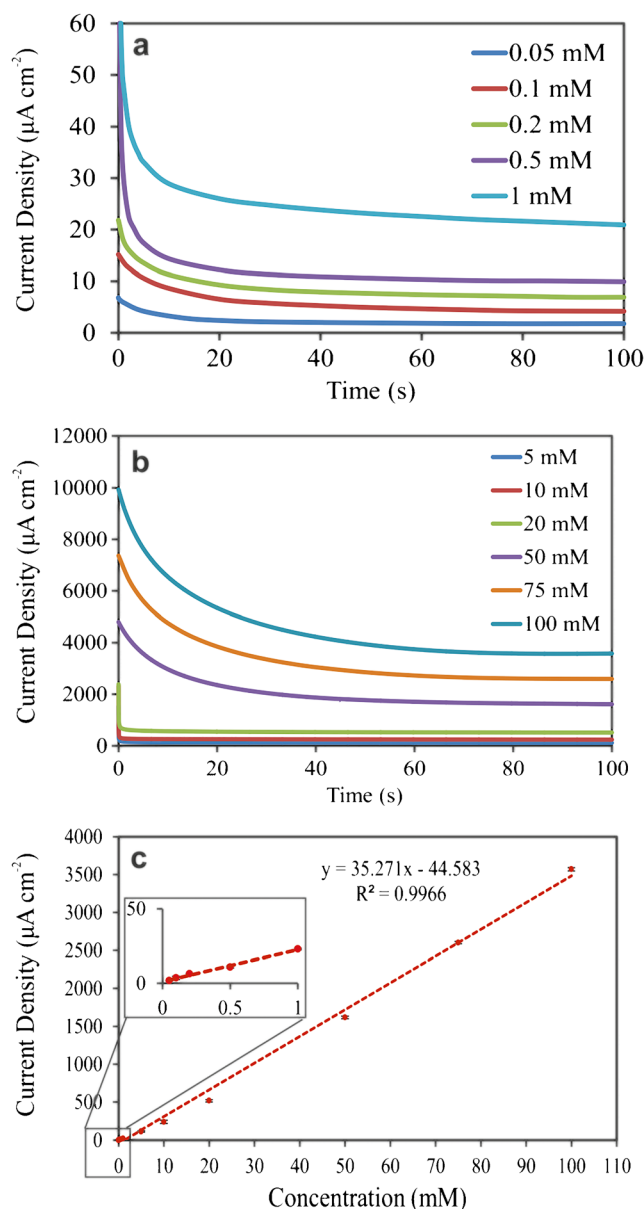


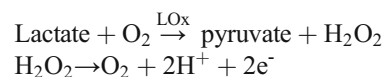
**Fig. 3** Electrochemical analysis of nanobiosensor panels **a** and **b** represent the amperometric responses towards the varying concentrations of lactic acid in the 0.1 M phosphate buffer (pH = 7.5) at 0.2 V **c** The calibration plot based on amperometric responses at different concentrations of lactic acid in the phosphate buffer after 80 s

**Table 1** Comparison of the analytical performance of the new biosensor with other electrochemical lactate biosensors

Electrode material	Linear range (mM)	Detection limit ( $\mu\text{M}$ )	Sensitivity	References
LOx/AuNP/CNT/Gr/Pt	0.05–100	2.3	35.3 ( $\mu\text{A mM}^{-1} \text{cm}^{-2}$ )	The present nanobiosensor
Ni-MOF <sup>a</sup> /Pt	0.01–0.9, 1–4	5.0	106.617, 29.533 ( $\mu\text{A mM}^{-1}$ )	[26]
Nafion/LOx/BSA <sup>b</sup> /GA <sup>c</sup> /Ag NP	1–25	–	0.262 ( $\mu\text{A mM}^{-1} \text{cm}^{-2}$ )	[27]
LOx/BSA/HRP <sup>d</sup> /CS <sup>e</sup> /FcMe <sup>f</sup> /MWCNT/SPBGE <sup>g</sup>	0.0304–0.2439	22.6	3.417 ( $\mu\text{A mM}^{-1}$ )	[28]
LDH/NAD <sup>+</sup> /pTTC <sup>h</sup> /MWCNT/Au	0.005–0.09	1.0	0.0106 ( $\mu\text{A mM}^{-1}$ )	[12]
LDH/MWCNT-MB <sup>k</sup>	0.10–10	7.5	3.46 ( $\mu\text{A mM}^{-1} \text{cm}^{-2}$ )	[11]
PDDA <sup>l</sup> /LOx/ZnO/MWCNT	0.2–2.0	6.0	7.3 $\mu\text{A mM}^{-1}$	[14]
LOx/ZnO nanotetrapod/Au	0.0036–0.6	1.2	28 ( $\mu\text{A mM}^{-1} \text{cm}^{-2}$ )	[15]
LOx/N-CNT <sup>m</sup> /GC <sup>n</sup>	0.014–0.325	4.1	40 ( $\mu\text{A mM}^{-1} \text{cm}^{-2}$ )	[29]

<sup>a</sup> Nickel-metal organic framework<sup>b</sup> Bovine serum albumin<sup>c</sup> Glutaraldehyde<sup>d</sup> Horseradish peroxidase<sup>e</sup> Chitosan<sup>f</sup> Ferrocene methanol.<sup>g</sup> Screen-printed graphite electrode<sup>h</sup> Nicotinamide adenine dinucleotide<sup>i</sup> Poly-5, 2'-5',2''-terthiophene-3'-carboxylic acid<sup>k</sup> Meldola blue<sup>l</sup> Polydiallyldimethylammonium chloride<sup>m</sup> Nitrogen-doped carbon nanotubes<sup>n</sup> Glassy carbon

The LOx, as a receptor in this work, can catalyze the oxidation reaction of lactate into pyruvate on the electrode surface as shown in the following reactions:



The generated hydrogen peroxide is simultaneously involved in the oxidation reaction that is associated with the electron production [15]. These electrons are detectable using various electrochemical techniques [16, 25].

The electrode surface was separately modified with the rGO, the rGO-CNT and the rGO-CNT-Au nanocomposite in order to investigate the effects of each nanostructure on

electrocatalytic activity, the electron transfer kinetics and the enzyme loading on the electrode. Figure 2b shows the CV curves of three sensors (LOx/rGO/Pt, LOx/CNT/rGO/Pt and LOx/Au/CNT/rGO/Pt) in the presence of 10 mM L-lactic acid in the phosphate buffer (pH = 7.5) at the scan rate of 0.1 V. The comparison of the CVs revealed the important role of each component of the nanocomposite. The GO-CNT hybrid acted as good support for the growth of AuNPs, through the anchoring of Au<sup>3+</sup> ions with the functional groups of GO, to provide the required surface for a maximum enzyme loading. The CNTs and AuNPs were found to accelerate the electron transfer process between the active site of the enzyme and the surface of the electrode. This results in a considerable increase in the current. Increasing the amount of enzyme loaded on the

**Table 2** Lactate determination in real samples

Sample	Average value of measured lactate concentration (mM)	RSD (%)
Milk	6.56	1.21 × 10 <sup>-1</sup>
Blood (before exercise, normoxia conditions)	1.45	3.80 × 10 <sup>-1</sup>
Blood (after exercise, hypoxia conditions)	1.49	1.23
Cell culture media (cultured in normoxia conditions)	2.64	0.50 × 10 <sup>-1</sup>
Cell culture media (cultured in hypoxia conditions)	2.67	2.20 × 10 <sup>-1</sup>

All the experiments were performed in triplicates

**Table 3** The recovery analysis of the sensor

Original (mM)	Addition (mM)	Detection (average, mM)	Recovery (%)	RSD (%)
1.45	1.00	2.42	97.00	2.07
–	1.70	3.23	104.71	$7.7 \times 10^{-1}$
–	2.30	3.71	98.26	1.54

The recovery analyses were performed in triplicates

electrode surface and accelerating the electron transfer improve sensitivity and linearity. Figure 2b illustrates that AuNPs shift the oxidation peak to lower potentials and improve the sensitivity and limit of detection (LOD), in large part due to strong electrocatalytic activity.

### Optimization of conditions

The following parameters were optimized: (a) sample pH value; (b) polarization voltage; (c) detection technique (Fig. S1, Electronic Supporting Materials). The following experimental conditions were found to provide: (a) the best sample pH value at 7.5; (b) the optimal polarization potential at 0.2 V; (c) the most applicable detection technique, i.e., amperometry.

### Analytical performance

The amperometric responses of the working electrode towards the varying concentrations of lactate in the 0.1 M phosphate buffer (pH = 7.5) at a potential of 0.2 V were recorded using a 2 mm diameter nanocomposite modified electrode. Figure 3a,b illustrates that the currents reached stable values for all concentrations after an 80 s period. Based on the recorded amperometric responses to different lactate concentrations ( $n = 5$ ), the calibration plot was obtained (Fig. 3c). The results exhibited a wide linear range of 0.05–100 mM concentration of lactate with a LOD of 2.3  $\mu\text{M}$  and sensitivity of 35.3  $\mu\text{A mM}^{-1} \text{cm}^{-2}$ .

The selectivity was evaluated by the analysis of the nanobiosensor responses to the presence of several common interfering substances such as glucose, fructose, ascorbic acid, dopamine and uric acid in biological concentrations. As shown in Fig. S2 (Electronic Supporting Materials), our findings demonstrated that the effect of the addition of glucose and fructose (10 mM), uric acid (saturation concentration in the phosphate buffer), dopamine and ascorbic acid (1 mM, more than the concentrations in milk and or physiological levels in the blood) is negligible on the signal towards 10 mM lactate solution. Such an excellent selectivity for lactate (at 0.2 V) might be attributed to the specific interaction between the LOx and lactate molecules.

The responses to 10 mM lactate over 20 detections exhibited excellent repeatability with a relative standard deviation (RSD) of 2.2%. The measurement of the lactate concentration

(10 mM in the phosphate buffer) with 10 nanocomposite modified electrodes indicated a good reproducibility for sensor fabrication ( $n = 3$ , RSD = 1.9%). Moreover, the monitoring of the electrode responses to 10 mM lactate during one-month storage period at 4 °C indicated that the sensor fully retains its initial response current, indicating excellent storage stability.

Table 1 compares the analytical parameters of the biosensor with other electrochemical biosensors used for the detection of lactate. The results exhibited a simultaneous improvement in the linear range, sensitivity and comparable LODr in comparison with other lactate biosensors.

### Real sample analysis

The practical sensing ability of the electrode for the lactate was further investigated and proven in the milk, blood and cell culture media samples (Table 2). The results indicated that the sensor possesses a significant potential to measure the lactate levels in the food and biological samples under normoxic and hypoxic conditions. Moreover, we have also quantitatively modeled the effects of the hypoxia on the lactate production from the perspective of the molecular systems biology (our unpublished data). The mathematical analyses also showed an increase in the lactate levels under hypoxic condition. Table 2 shows that the sensor displays high sensitivity for the lactate detection in some real samples. It can detect the changes in the lactate concentrations in the human blood during exercise as well as the cell culture media during hypoxic conditions.

To evaluate the accuracy of the performance, different amounts of lactate were added to the blood sample and the recovery tests were carried out. As shown in Table 3, the recovery range was found to be from 97.00% to 104.71%, which confirms the capability of the sensor in the analysis of the real samples with high accuracy and excellent sensitivity.

### Conclusion

A nanocomposite of type rGO-CNT-Au was used to develop a novel biosensor for lactate with high sensitivity and wide linear range. The nanocomposite was synthesized through  $\text{Au}^{3+}$  reduction on the rGO-CNT hybrid and characterized by EDX,

XRD, TEM and electrochemical techniques. As a result, a Pt electrode modified with the rGO-CNT-Au nanocomposite and LOx was established. The use of three components of the nanocomposite resulted in an excellent synergistic effect on the performance. The nanobiosensor displayed a high performance in terms of lactate detection in the real samples even within complex matrix under both normoxic and hypoxic conditions. Taken all, the sensor is shown to serve as a highly sensitive, yet simple and cost-effective, tool for the detection of lactate. We envision that the replacement of the disk electrodes with the screen-printed electrodes can turn the nanobiosensor to a portable and user-friendly system for the screening of lactate in various samples. Furthermore, the rGO-CNT-Au nanocomposite is suggested to be used for the immobilization of different biomolecules in the development of various electrochemical nanobiosensors.

**Acknowledgments** This article is a part of a Ph.D. thesis, written by Ms. Shabnam Hashemzadeh, approved at the School of Medicine, Shahid Beheshti University of Medical Sciences, Tehran-Iran (Registration No: M 360) in collaboration with the Research Center for Pharmaceutical Nanotechnology (RCPN) at Tabriz University of Medical Sciences, Tabriz-Iran. This study was financially supported by and technically conducted at the RCPN (Grant No: 97005).

### Compliance with ethical standards

**Conflict of interests** The authors declare no conflict of interests.

**Ethical issues** This study was ethically approved by Shahid Beheshti University of Medical Sciences (Approval ID: IR.SBMU.MSP.REC.1396.753).

### References

- Barar J, Omid Y (2013) Dysregulated pH in tumor microenvironment checkmates cancer therapy. *BioImpacts*. 3(4):149–162. <https://doi.org/10.5681/bi.2013.036>
- Katz A, Sahlin K (1987) Effect of decreased oxygen availability on NADH and lactate contents in human skeletal muscle during exercise. *Acta Physiol Scand* 131(1):119–127. <https://doi.org/10.1111/j.1748-1716.1987.tb08213.x>
- Lum JJ, Bui T, Gruber M, Gordan JD, DeBerardinis RJ, Covellos KL et al (2007) The transcription factor HIF-1 $\alpha$  plays a critical role in the growth factor-dependent regulation of both aerobic and anaerobic glycolysis. *Genes Dev* 21(9):1037–1049. <https://doi.org/10.1101/gad.1529107>
- Annibaldi A, Widmann C (2010) Glucose metabolism in cancer cells. *Curr Opin Clin Nutr Metab Care* 13(4):466–470. <https://doi.org/10.1097/MCO.0b013e32833a5577>
- Bartrons R, Caro J (2007) Hypoxia, glucose metabolism and the Warburg's effect. *J Bioenerg Biomembr* 39(3):223–229. <https://doi.org/10.1007/s10863-007-9080-3>
- Goodwin ML, Gladden LB, Nijsten MW, Jones KB (2015) Lactate and cancer: revisiting the Warburg effect in an era of lactate shuttling. *Frontiers Nutr* 1:1–3. <https://doi.org/10.3389/fnut.2014.00027>
- Rathee K, Dhull V, Dhull R, Singh S (2016) Biosensors based on electrochemical lactate detection: a comprehensive review. *Biochem Biophys Rep* 5:35–54. <https://doi.org/10.1016/j.bbrep.2015.11.010>
- Pal R, Parker D, Costello LC (2009) A europium luminescence assay of lactate and citrate in biological fluids. *Org Biomol Chem* 7(8):1525–1528. <https://doi.org/10.1039/b901251f>
- Sartain FK, Yang X, Lowe CR (2006) Holographic lactate sensor. *Anal Chem* 78(16):5664–5670. <https://doi.org/10.1021/ac060416g>
- Takahashi S, Kurosawa S (2008) Anzai Ji. Electrochemical determination of L-lactate using Phenylboronic acid monolayer-modified electrodes. *Electroanalysis*. 20(7):816–818. <https://doi.org/10.1002/elan.200704097>
- Pereira AC, Aguiar MR, Kisner A, Macedo DV, Kubota LT (2007) Amperometric biosensor for lactate based on lactate dehydrogenase and Meldola blue coimmobilized on multi-wall carbon-nanotube. *Sensors Actuators B Chem* 124(1):269–276. <https://doi.org/10.1016/j.snb.2006.12.042>
- Rahman M, Shiddiky MJ, Rahman MA, Shim Y-B (2009) A lactate biosensor based on lactate dehydrogenase/nicotinamide adenine dinucleotide (oxidized form) immobilized on a conducting polymer/multiwall carbon nanotube composite film. *Anal Biochem* 384(1):159–165. <https://doi.org/10.1016/j.ab.2008.09.030>
- Sirkar K, Revzin A, Pishko MV (2000) Glucose and lactate biosensors based on redox polymer/oxidoreductase nanocomposite thin films. *Anal Chem* 72(13):2930–2936. <https://doi.org/10.1021/ac991041k>
- Wang Y, Bao Y, Lou L, Li J, Du W, Zhu Z et al (2010) A novel L-lactate sensor based on enzyme electrode modified with ZnO nanoparticles and multiwall carbon nanotubes. *J Electroanal Chem*:33–37. <https://doi.org/10.1016/j.jelechem.2011.06.024>
- Lei Y, Luo N, Yan X, Zhao Y, Zhang G, Zhang Y (2012) A highly sensitive electrochemical biosensor based on zinc oxide nanotetrapods for L-lactic acid detection. *Nanoscale*. 4(11):3438–3443. <https://doi.org/10.1039/C2NR30334E>
- Ibupoto ZH, Shah SMUA, Khun K, Willander M (2012) Electrochemical L-lactic acid sensor based on immobilized ZnO nanorods with lactate oxidase. *Sensors*. 12(3):2456–2466. <https://doi.org/10.3390/s120302456>
- Zhao Y, Li W, Pan L, Zhai D, Wang Y, Li L et al (2016) ZnO-nanorods/graphene heterostructure: a direct electron transfer glucose biosensor. *Sci Rep* 6:32327. <https://doi.org/10.1038/srep32327>
- Zhang W, Li X, Zou R, Wu H, Shi H, Yu S et al (2015) Multifunctional glucose biosensors from Fe<sub>3</sub>O<sub>4</sub> nanoparticles modified chitosan/graphene nanocomposites. *Sci Rep* 5:11129. <https://doi.org/10.1038/srep32327>
- Song J, Xu L, Xing R, Li Q, Zhou C, Liu D et al (2014) Synthesis of Au/graphene oxide composites for selective and sensitive electrochemical detection of ascorbic acid. *Sci Rep* 4:7515. <https://doi.org/10.1038/srep07515>
- Rakhi R, Nayak P, Xia C, Alshareef HN (2016) Novel amperometric glucose biosensor based on MXene nanocomposite. *Sci Rep* 6:36422. <https://doi.org/10.1038/srep32327>
- Hossain MF, Park JY (2016) Plain to point network reduced graphene oxide-activated carbon composites decorated with platinum nanoparticles for urine glucose detection. *Sci Rep* 6:21009. <https://doi.org/10.1038/srep21009>
- Wang J (2005) Carbon-nanotube based electrochemical biosensors: a review. *Electroanalysis*. 17(1):7–14. <https://doi.org/10.1002/elan.200403113>
- Nikoleli G-P, Karapetis S, Bratakou S, Nikolelis DP, Tzamtzis N, Psychoyios VN (2016) Graphene-based electrochemical

- biosensors: new trends and applications. *Intelligent Nanomat* 2: 427–448. <https://doi.org/10.1002/9781119242628.ch13>
24. Marcano DC, Kosynkin DV, Berlin JM, Sinititskii A, Sun Z, Slesarev A et al (2010) Improved synthesis of graphene oxide. *ACS Nano* 4(8):4806–4814. <https://doi.org/10.1021/nn1006368>
  25. Hwa K-Y, Subramani B (2014) Synthesis of zinc oxide nanoparticles on graphene–carbon nanotube hybrid for glucose biosensor applications. *Biosens Bioelectron* 62:127–133. <https://doi.org/10.1016/j.bios.2014.06.023>
  26. Perumal M, Nesakumar N, Velayutham D, Madasamy K, Murugavel K, Kulandaisamy AJ et al (2018) A novel electrochemical sensor based on a nickel-metal organic framework for efficient electrocatalytic oxidation and rapid detection of lactate analysis. *New J Chem* 42:11839–11846. <https://doi.org/10.1039/c8nj02118j>
  27. Abrar MA, Dong Y, Lee PK, Kim WS (2016) Bendable electrochemical lactate sensor printed with silver nano-particles. *Sci Rep* 6:30565. <https://doi.org/10.1038/srep30565>
  28. Hernández-Ibáñez N, García-Cruz L, Montiel V, Foster CW, Banks CE, Iniesta J (2016) Electrochemical lactate biosensor based upon chitosan/carbon nanotubes modified screen-printed graphite electrodes for the determination of lactate in embryonic cell cultures. *Biosens Bioelectron* 77:1168–1174. <https://doi.org/10.1016/j.bios.2015.11.005>
  29. Goran JM, Lyon JL, Stevenson KJ (2011) Amperometric detection of l-lactate using nitrogen-doped carbon nanotubes modified with lactate oxidase. *Anal Chem* 83(21):8123–8129. <https://doi.org/10.1021/ac2016272>

**Publisher's note** Springer Nature remains neutral with regard to jurisdictional claims in published maps and institutional affiliations.